Inorg. Chem. **2006**, *45*, 10976–10989

Copper(II) Complexes of salen Analogues with Two Differently Substituted (Push–Pull) Salicylaldehyde Moieties. A Study on the Modulation of Electronic Asymmetry and Nonlinear Optical Properties

Luca Rigamonti,[†] Francesco Demartin,*[,‡] Alessandra Forni,*[,§] Stefania Righetto,[†] and Alessandro Pasini*[,†]

Dipartimento di Chimica Inorganica, Metallorganica e Analitica, and Dipartimento di Chimica Strutturale e Stereochimica Inorganica, Università degli Studi di Milano, via G. Venezian 21, 20133 Milano, Italy, and CNR-ISTM, via Golgi 19, 20133 Milano, Italy

Received July 20, 2006

This paper presents some copper(II) complexes of salen analogues in which the two salicylaldehyde moieties carry different (electron donor, D, and acceptor, A) substituents in position 5, producing a push–pull charge asymmetry. The X-ray structures of some compounds show the presence of pairs of stacked molecules with head-to-tail intermolecular associations. The geometries of all complexes have been optimized through density functional theory (DFT) studies, which have shown that a major influence on the coordination bond lengths is given by the presence of the electron acceptor NO_2 group. Such an influence operates mainly on the Cu–phenolato bonds: elongation of the Cu–O distance of the 5-nitrosalicylaldehyde moiety, with a concomitant decrease of the other Cu–O distance; the Cu–N bonds are less affected. The D groups have only a minor influence. The nonlinear optical responses, $\mu_g\beta_{vec}$, of some molecules have been determined by EFISH measurements, and the β_{vec} values have been obtained using the DFT-calculated μ_g values because solubility problems hampered the experimental measurements of μ_g of some derivatives; the former, however, have been found to be in agreement with the experimental values that could be obtained. Deconvolution of the absorption bands in the near-UV region has allowed recognition of the charge-transfer (CT) transition, assigned to a ligand-to-metal CT (LMCT) by time-dependent DFT computations; we have then used the solvatochromism of this transition to obtain β_0 and β_{CT} values using the two-state model. These values were compared with those obtained by computational studies, which have also allowed evaluation of the influence of the substituents on the directions of μ_g and β_{tot}.

Introduction

The growing interest in nonlinear optics has led to the synthesis of new compounds and materials. Among the molecular compounds that display nonlinear optical (NLO) behavior, molecules with a D$-\pi-$A structure have been studied in great detail.[1] These molecules are polarizable, noncentrosymmetric systems in which an electron donor, D, group and an electron acceptor, A, group are linked through a delocalized π system, which provides the polarizable electrons.

More recently, organometallic and coordination compounds have been actively investigated because they offer a large variety of molecular structures and electronic properties, as well as the possibility of "switching on", or enhancing, the NLO properties of the organic ligands through complexation to a metal center.[2−5] Complexes of Schiff bases of the salen type are particularly interesting in these respects[6] because of their thermal stability, the active role of the metal center (oxidation state and d configuration) as a bridge between the A and D groups, and the presence of charge-transfer (CT) transitions at low energies.

The microscopic polarization of a molecule is given by the power series in the field strength **E**:

$$\mathbf{P} = \alpha\mathbf{E} + \beta\mathbf{EE} + \gamma\mathbf{EEE} + ...$$

where α is the linear polarizability and β and γ are the quadratic and cubic hyperpolarizabilities, respectively. The

* To whom correspondence should be addressed. E-mail: francesco.demartin@unimi.it (F.D.), a.forni@istm.cnr.it (A.F.), alessandro.pasini@unimi.it (A.P.).
[†] Dipartimento di Chimica Inorganica, Metallorganica e Analitica, Università degli Studi di Milano.
[‡] Dipartimento di Chimica Strutturale e Stereochimica Inorganica, Università degli Studi di Milano.
[§] CNR-ISTM.

10.1021/ic0613513 CCC: $33.50
Published on Web 12/06/2006

Chart 1

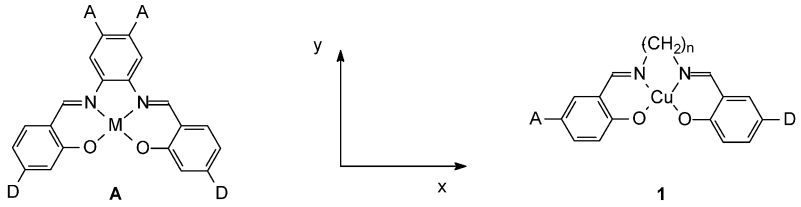

A **1**

numb.	**1a**	**1b**	**1c**	**1d**	**1e**	**1f**	**1g**	**1h**	**1i**	**1j**	**1k**	**1l**	**1m**	**1n**	**1o**	**1p**
n	2	2	2	2	2	2	2	2	3	3	3	3	3	3	3	3
A	H	H	H	H	NO_2	NO_2	NO_2	NO_2	H	H	H	H	NO_2	NO_2	NO_2	NO_2
D	H	Me	OMe	NMe_2	H	Me	OMe	NMe_2	H	Me	OMe	NMe_2	H	Me	OMe	NMe_2

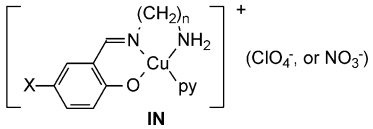

IN

numb.	**IN1**	**IN2**	**IN3**	**IN4**
n	2	2	3	3
X	H	NO_2	H	NO_2

β tensor is responsible for the second-order NLO response. The NLO properties, in particular β_{vec} (where β_{vec} is the projection of β_{tot}, i.e., the vectorial part of β, along the direction of the ground-state dipole moment, μ_g), of these materials are enhanced in complexes of type **A** (see Chart 1), where the presence of D groups in position 4 of salicylaldehyde (hereafter sal) and A groups on the diamine increases the charge asymmetry along the *y* axis of the [M(salen)] structure.[6,7] In an attempt to increase the scope of salen-type complexes, we wanted to study the effect of charge asymmetry along the *x* axis, obtained by use of salen analogues in which the two salicylaldehyde moieties bear different substituents in position 5 (see complexes **1** in Chart 1). In particular, our interest was to investigate the effect of such charge asymmetry on coordination bond lengths and on the electronic and nonlinear optical properties. This approach is independent of the diamine and, because of the possibility of a variety of substitutions, has a rich potential of fine-tuning the molecular properties.

This paper therefore reports the syntheses of copper(II) complexes **1** (performed through intermediates **IN**, also presented in Chart 1), the X-ray structural determinations of **1g**, **1n**, **1o**, and **1p**, and the optimized geometries of all compounds, obtained by density functional theory (DFT) computational studies. The electronic properties of the compounds, in particular the nature of the CT states, will be elucidated through a detailed analysis of their electronic spectra. In addition, we report the values of the first hyperpolarizability of selected compounds, obtained both experimentally (EFISH and solvatochromic measurements) and by DFT studies. The latter were undertaken also to determine the influence of the push−pull asymmetry along the *x* axis on the tilting of the dipole moments and the β_{tot} vectors from the *y* direction, which is intrinsic of the parent [Cu(salen)] (**1a**).

The theoretical description of the electronic properties of open-shell systems, such as d^9 copper(II) complexes, represents a nontrivial problem in quantum chemistry, in particular as far as the determination of the excited-state and NLO

(1) (a) Prasad, P. N.; Williams, D. J. *Introduction to nonlinear optical effects in molecules and polymers*; Wiley: New York, 1991. (b) Marder, S. R.; Sohn, J. E.; Stucky, G. D. *Materials for Nonlinear Optics: Chemical Perspectives*; ACS Symposium Series 455; American Chemical Society: Washington, DC, 1991. (c) Marder, S. R. *Chem. Commun.* **2006**, 131−134. (d) Leclerc, N.; Sanaur, S.; Galmiche, L.; Mathevet, F.; Attias, A.-J.; Fave, J.-L.; Roussel, J.; Hapiot, P.; Lemaître, N.; Geffroy, B. *Chem. Mater.* **2005**, *17*, 502−513. (e) Cole, J. M.; Kreiling, S. *CrystEngComm* **2002**, *4*, 232−238. (f) Ostroverkhov, V.; Petschek, R. G.; Singer, K. D.; Twieg, R. J. *Chem. Phys. Lett.* **2001**, *340*, 109−115. (g) Kanis, D. R.; Ratner, M. A.; Marks, T. J. *Chem. Rev.* **1994**, *94*, 195−242. (h) Nie, W. *Adv. Mater.* **1993**, *5*, 520−545. (i) Kuzyk, M. G.; Eich, M.; Norwood, R. A. *Linear and Nonlinear Optics of Organic Materials III*; Proceedings of SPIE; SPIE: San Diego, CA, August 2003; pp 4−8.

(2) (a) Di Bella, S. *Chem. Soc. Rev.* **2001**, *30*, 355−366. (b) Coe, B. J.; Curati, N. R. M. *Comments Inorg. Chem.* **2004**, *25*, 147−184. (c) Le Bozec, H.; Renouard, T. *Eur. J. Inorg. Chem.* **2000**, 229−239. (d) Heck, J.; Dabek, S.; Meyer-Friedrichsen, T.; Wong, H. *Coord. Chem. Rev.* **1999**, *190*−*192*, 1217−1254. (e) Whittall, I. R.; McDonagh, A. M.; Humphrey, M. G.; Samoc, M. *Adv. Organomet. Chem.* **1998**, *42*, 291−362. (f) Long, N. J. *Angew. Chem., Int. Ed. Engl.* **1995**, *34*, 21−38. (g) Powell, C. P.; Humphrey, M. G.; Morrall, J. P. L.; Samoc, M.; Luther-Davies, B. *J. Phys. Chem. A* **2003**, *107*, 11264−11266.

(3) (a) Kanis, D. R.; Lacroix, P. G.; Ratner, M. A.; Marks, T. J. *J. Am. Chem. Soc.* **1994**, *116*, 10089−10102. (b) Roberto, D.; Ugo, R.; Bruni, S.; Cariati, E.; Cariati, F.; Fantucci, P.; Invernizzi, I. *Organometallics* **2000**, *19*, 1775−1788. (c) Di Bella, S.; Fragalà, I.; Ledoux, I.; Zyss, J. *Chem.*−*Eur. J.* **2001**, *7*, 3738−3743. (d) Lenoble, G.; Lacroix, P. G.; Daran, J. C.; Di Bella, S.; Nakatani, K. *Inorg. Chem.* **1998**, *37*, 2158−2165.

(4) (a) Qin, J.; Liu, D.; Dai, C.; Chen, C.; Wu, B.; Yang, C.; Zhan, C. *Coord. Chem. Rev.* **1999**, *188*, 23−34. (b) Costes, J. P.; Lamère, J. F.; Lepetit, C.; Lacroix, P. G.; Dahan, F.; Nakatani, K. *Inorg. Chem.* **2005**, *44*, 1973−1982. (c) Lacroix, P. G.; Averseng, F.; Malfant, I.; Nakatani, K. *Inorg. Chim. Acta* **2004**, *357*, 3825−3835. (d) Margeat, O.; Lacroix, P. G.; Costes, J. P.; Donnadieu, B.; Lepetit, C.; Nakatani, K. *Inorg. Chem.* **2004**, *43*, 4743−4750. (e) Averseng, F.; Lacroix, P. G.; Malfant, I.; Périssé, N.; Lepetit, C.; Nakatani, K. *Inorg. Chem.* **2001**, *40*, 3797−3804. (f) Averseng, F.; Lepetit, C.; Lacroix, P. G.; Tuchagues, J. P. *Chem. Mater.* **2000**, *12*, 2225−2229.

(5) (a) Di Bella, S.; Fragalà, I.; Ledoux, I.; Marks, T. J. *J. Am. Chem. Soc.* **1995**, *117*, 9481−9485. (b) Di Bella, S.; Fragalà, I.; Marks, T. J.; Ratner, M. A. *J. Am. Chem. Soc.* **1996**, *118*, 12747−12751. (c) Di Bella, S.; Fragalà, I.; Guerri, A.; Dapporto, P.; Nakatani, K. *Inorg. Chim. Acta* **2004**, *357*, 1161−1167.

(6) (a) Lacroix, P. G. *Eur. J. Inorg. Chem.* **2001**, 339−348. (b) Di Bella, S.; Fragalà, I. *Synth. Met.* **2000**, *115*, 191−196. (c) Lacroix, P. G. *Lett. Sci. Chim.* **1999**, *68*, 35−37.

(7) (a) Di Bella, S.; Fragalà, I. *New J. Chem.* **2002**, *26*, 285−290. (b) Lacroix, P. G.; Di Bella, S.; Ledoux, I. *Chem. Mater.* **1996**, *8*, 541−545.

properties is concerned (see, for instance, ref 8 and references cited therein). DFT and its time-dependent extension (TD-DFT) have shown to accurately evaluate a variety of ground- and excited-state properties of large systems, in particular of transition-metal complexes.[9] Very few applications have, however, been devoted to the study of NLO properties of open-shell systems and, to our knowledge, most of them were performed using semiempirical methods.[5] Our results obtained from first principles (ab initio) calculations provide a reliable description of both structural and excited-state properties of the complexes, as well as of their NLO properties, allowing rationalization and substantiation of the experimental findings.

Experimental Section

General Procedures. All chemicals were reagent grade. Solvents were used as received. 5-(Dimethylamino)salicylaldehyde was synthesized from 5-nitrosalicylaldehyde following a published procedure.[10]

Elemental analyses were performed at the Microanalytical Laboratory at our university. Fast atom bombardment mass spectrometry (FAB-MS) spectra were recorded on a VCA Analytical 7070 EQ instrument. Dipolar moments were obtained with the Guggenheim method,[11] using a WTW DM01 dipolemeter and an ATAGO RX-5000 refractometer.

Synthesis of Intermediates.[12] ***Caution!*** *Perchlorate salts of metal complexes with organic ligands are potentially explosive and must be handled with care and in small amounts.*

IN1ClO$_4$. An aqueous solution of Cu(ClO$_4$)$_2$·6H$_2$O (1.500 g, 4 mmol in 5 mL) was added to a stirred solution of salicylaldehyde (0.490 g, 4 mmol) in methanol (10 mL) followed by pyridine (0.6 mL, 8 mmol). The mixture was stirred at room temperature for 1 h, and then 0.240 g (4 mmol) of ethylenediamine was added. After 3 h at room temperature, the dark-violet solid was filtered, washed with methanol and diisopropyl ether, and dried in vacuo (1.260 g, 75%). Anal. Calcd for $C_{14}H_{16}N_3O_5CuCl$ (405.30): C, 41.49; H, 3.98; N, 10.37. Found: C, 41.63; H, 4.09; N, 10.53. IR (KBr): 3324, 3269 (ν_{NH_2}), 1632 ($\nu_{C=N}$) cm^{-1}. FAB-MS: *m*/*z* 226 [M − py$^+$].

IN2NO$_3$. This green compound was prepared as above, using 0.700 g of Cu(NO$_3$)$_2$·2.5H$_2$O (3 mmol in 5 mL of water), 0.500 g of 5-nitrosalicylaldehyde (3 mmol) in 20 mL of methanol, 0.49 mL of pyridine (6 mmol), and 0.180 g of ethylenediamine (3 mmol). Yield: 1.110 g, 90%. Anal. Calcd for $C_{14}H_{15}N_5O_6Cu$ (412.85): C, 40.73; H, 3.66; N, 16.96. Found: C, 40.84; H, 3.58; N, 17.06. IR (KBr): 3313, 3231 (ν_{NH_2}), 1653 ($\nu_{C=N}$), 1317 (ν_{NO_2}) cm^{-1}. FAB-MS: *m*/*z* 271 [M − py$^+$].

IN3ClO$_4$. This dark-green compound was prepared by the same method starting from a 5-mL aqueous solution of 1.500 g of Cu(ClO$_4$)$_2$·6H$_2$O (4 mmol), 0.490 g of salicylaldehyde (4 mmol) in 10 mL of methanol, 0.65 mL of pyridine (8 mmol), and 0.297 g of 1,3-diaminopropane (4 mmol). Yield: 1.430 g, 84%. Anal. Calcd for $C_{15}H_{18}N_3O_5CuCl$ (419.32): C, 42.97; H, 4.33; N, 10.02. Found: C, 42.60; H, 4.02; N, 9.87. IR (KBr): 3315, 3256 (ν_{NH_2}), 1631 ($\nu_{C=N}$) cm^{-1}. FAB-MS: *m*/*z* 240 [M − py$^+$].

IN4ClO$_4$. 5-Nitrosalicylaldehyde (0.550 g, 3.3 mmol) and NaOH (3.3 mL of a 1 mol L^{-1} ethanol solution) were mixed in methanol (20 mL) followed by the addition of an aqueous (5 mL) solution of Cu(ClO$_4$)$_2$·6H$_2$O (1.215 g, 3.3 mmol) and pyridine (0.53 mL, 6.6 mmol). The slurry was stirred at room temperature for 1 h, and then 1,3-diaminopropane (0.245 g, 3.3 mmol) was added. The dark-green product was filtered off after 3 h, washed with methanol and diisopropyl ether, and dried in vacuo (1.310 g, 86%). Anal. Calcd for $C_{15}H_{17}N_4O_7CuCl$ (464.32): C, 38.80; H, 3.69; N, 12.07. Found: C, 38.94; H, 3.50; N, 12.28. IR (KBr): 3313, 3253 (ν_{NH_2}), 1629 ($\nu_{C=N}$), 1318 (ν_{NO_2}) cm^{-1}. FAB-MS: *m*/*z* 285 [M − py$^+$].

Synthesis of Compounds 1. 1a and **1i** were prepared according to a standard procedure.[13]

1b. Solid **IN1**ClO$_4$ (0.405 g, 1 mmol) was added to a stirred solution of 5-methylsalicylaldehyde (0.163 g, 1.2 mmol) in methanol (10 mL) and 1.2 mL of 1 mol L^{-1} aqueous NaOH. The mixture was refluxed for 30 min and cooled, and the filtered product was washed with methanol and diisopropyl ether and dried in vacuo (0.300 g, 87%). Anal. Calcd for $C_{17}H_{16}N_2O_2Cu$ (343.87): C, 59.38; H, 4.69; N, 8.15. Found: C, 59.39; H, 4.90; N, 8.19. IR (KBr): 1649, 1632 ($\nu_{C=N}$) cm^{-1}. FAB-MS: *m*/*z* 344 [M + H$^+$].

The other complexes **1c**−**1h** and **1j**−**1p** were obtained with the same procedure using the appropriate intermediate **IN** and various salicylaldehydes.

1c. From **IN1** and 5-methoxysalicylaldehyde (0.263 g, 73%). Anal. Calcd for $C_{17}H_{16}N_2O_3Cu$ (359.87): C, 56.74; H, 4.48; N, 7.78. Found: C, 56.68; H, 4.55; N, 7.78. IR (KBr): 1648, 1635 ($\nu_{C=N}$) cm^{-1}. FAB-MS: *m*/*z* 360 [M + H$^+$].

1d. From **IN1** and 5-(dimethylamino)salicylaldehyde (0.242 g, 65%). Anal. Calcd for $C_{18}H_{19}N_3O_2Cu$ (372.92): C, 57.98; H, 5.14; N, 11.27. Found: C, 57.78; H, 4.97; N, 11.12. IR (KBr): 1634 ($\nu_{C=N}$) cm^{-1}. FAB-MS: *m*/*z* 373 [M + H$^+$].

1e. From **IN1** and 5-nitrosalicylaldehyde (0.361 g, 92%). Anal. Calcd for $C_{16}H_{13}N_3O_4Cu·H_2O$ (392.86): C, 48.92; H, 3.85; N, 10.70. Found: C, 48.93; H, 3.62; N, 10.86. IR (KBr): 1637 ($\nu_{C=N}$), 1309 (ν_{NO_2}) cm^{-1}. FAB-MS: *m*/*z* 375 [M + H$^+$].

1f. From **IN2** and 5-methylsalicylaldehyde (0.395 g, 97%). Anal. Calcd for $C_{17}H_{15}N_3O_4Cu·H_2O$ (406.89): C, 50.18; H, 4.21; N, 10.33. Found: C, 49.90; H, 4.48; N, 10.29. IR (KBr): 1636 ($\nu_{C=N}$), 1306 (ν_{NO_2}) cm^{-1}. FAB-MS: *m*/*z* 389 [M + H$^+$].

1g. From **IN2** and 5-methoxysalicylaldehyde (0.388 g, 96%). Anal. Calcd for $C_{17}H_{15}N_3O_5Cu$ (404.87): C, 50.43; H, 3.73; N, 10.38. Found: C, 50.52; H, 3.82; N, 10.38. IR (KBr): 1636 ($\nu_{C=N}$), 1303 (ν_{NO_2}) cm^{-1}. FAB-MS: *m*/*z* 405 [M + H$^+$].

1h. From **IN2** and 5-(dimethylamino)salicylaldehyde (0.393 g, 92%). Anal. Calcd for $C_{18}H_{18}N_4O_4Cu·{}^1/_2H_2O$ (426.92): C, 50.64; H, 4.48; N, 13.12. Found: C, 50.31; H, 4.33; N, 13.15. IR (KBr): 1636 ($\nu_{C=N}$), 1308 cm^{-1} (ν_{NO_2}). FAB-MS: *m*/*z* 417 [M$^+$].

(8) Grimme, S. Calculation of the Electronic Spectra of Large Molecules. In *Reviews in Computational Chemistry*; Lipkowitz, K. B., Larter, R., Cundari, T. R., Eds.; Wiley-VCH: New York, 2004; Vol. 20.

(9) (a) Koch, W.; Holthausen, M. C. *A Chemist's Guide to Density Functional Theory*, 2nd ed.; Wiley-VCH: New York, 2000. (b) Adamo, C.; di Matteo, A.; Barone, V. *Adv. Quantum Chem.* **1999**, *36*, 45−75. (c) Baerends, E. J.; Ricciardi, G.; Rosa, A.; van Gisbergen, S. J. A. *Coord. Chem. Rev.* **2002**, *230*, 5−27. (d) Hay, P. J. *J. Phys. Chem. A* **2002**, *106*, 1634−1641. (e) Hieringer, W.; Baerends, E. J. *J. Phys. Chem. A* **2006**, *110*, 1014−1021. (f) Bruschi, M.; Fantucci, P.; Pizzotti, M. *J. Phys. Chem. A* **2005**, *109*, 9637−9645. (g) Villegas, J. M.; Stoyanov, S. R.; Huang, W.; Rillema, D. P. *Inorg. Chem.* **2005**, *44*, 2297−2309. (h) De Angelis, F.; Fantacci, S.; Sgamellotti, A.; Cariati, F.; Roberto, D.; Tessore, F.; Ugo, R. *Dalton Trans*. **2006**, 852−859.

(10) Ando, M.; Emoto, S. *Bull. Chem. Soc. Jpn.* **1978**, *51*, 2433−2434.

(11) Guggenheim, E. A. *Trans. Faraday Soc.* **1949**, *45*, 714−720. Solubility problems hampered the measurements of many compounds.

(12) Costes, J.-P.; Dahan, F.; Fernandez Fernandez, M. B.; Fernendez Garcia, M. I.; Garcia Deibe, A. M.; Sanmartin, J. *Inorg. Chim. Acta* **1998**, *274*, 73−81.

(13) For instance, see: Downing, R. S.; Urbach, F. L. *J. Am. Chem. Soc.* **1969**, *91*, 5977−5983.

Table 1. Crystallographic Data

compd	**1g**	**1n**	**1o**	**1p**
formula	$C_{17}H_{15}CuN_3O_5$	$C_{36}H_{36}Cu_2N_6O_9$	$C_{19}H_{18}Cl_3CuN_3O_5$	$C_{20}H_{21}Cl_3CuN_4O_4$
fw (amu)	404.86	823.81	538.25	551.30
cryst syst	triclinic	triclinic	triclinic	monoclinic
space group	$P\bar{1}$ (No. 2)	$P\bar{1}$ (No. 2)	$P\bar{1}$ (No. 2)	$P2_1/n$ (No. 14)
a (Å)	8.699(2)	10.4644(5)	10.089(1)	17.093(3)
b (Å)	9.064(2)	13.7992(7)	11.347(1)	7.873(2)
c (Å)	11.094(2)	13.9798(7)	11.533(1)	17.254(4)
α (deg)	66.41(3)	113.91(1)	111.56(1)	90
β (deg)	80.23(3)	103.00(1)	105.25(1)	100.16(3)
γ (deg)	80.17(3)	96.08(1)	103.71(1)	90
V (Å^3)	785.0(3)	1753.6(3)	1099.7(2)	2285.5(8)
Z	2	2	2	4
D_{calcd} (g cm^{-3})	1.713	1.560	1.625	1.602
μ(Mo Kα) (mm^{-1})	1.428	1.278	1.394	1.342
θ range (deg)	1.0−26.0	1.0−26.0	1.0−26.0	1.0−24.0
indep reflns	3072	6783	4305	3282
obsd reflns [$I > 2\sigma(I)$]	2415	5244	2173	1.813
transmission factors	0.786−1.000	0.903−1.000	0.807−1.000	0.667−1.000
param refined	236	486	284	283
final R and R_w indices[a]	0.046, 0.108	0.036, 0.087	0.075, 0.216	0.060, 0.121
largest diff peak and hole (e Å^{-3})	0.68, −0.35	0.68, −0.31	0.84, −0.64	0.74, −0.90

[a] $R = [\sum(F_o - k|F_c|)/\sum F_o]$; $R_w = [\sum w(F_o - k|F_c|)^2/\sum wF_o^2]^{1/2}$.

1j. From **IN3** and 5-methylsalicylaldehyde (0.220 g, 57%). Anal. Calcd for $C_{18}H_{18}N_2O_2Cu\cdot{}^1/_3CH_2Cl_2$ (386.21): C, 57.01; H, 4.83; N, 7.25. Found: C, 56.71; H, 4.73; N, 7.07. IR (KBr): 1620 ($\nu_{C=N}$) cm^{-1}. FAB-MS: m/z 358 [M + H$^+$].

1k. From **IN3** and 5-methoxysalicylaldehyde (0.157 g, 40%). Anal. Calcd for $C_{18}H_{18}N_2O_3Cu\cdot H_2O$ (391.91): C, 55.16; H, 5.14; N, 7.15. Found: C, 55.12; H, 4.46; N, 7.21. IR (KBr): 1622 ($\nu_{C=N}$) cm^{-1}. FAB-MS: m/z 374 [M + H$^+$].

1l. From **IN3** and 5-(dimethylamino)salicylaldehyde (0.280 g, 64%). Anal. Calcd for $C_{19}H_{21}N_3O_2Cu\cdot CH_3OH\cdot H_2O$ (437.00): C, 54.97; H, 6.23; N, 9.62. Found: C, 54.60; H, 5.40; N, 9.89. IR (KBr): 1621 ($\nu_{C=N}$) cm^{-1}. FAB-MS: m/z 387 [M + H$^+$].

1m. From **IN3** and 5-nitrosalicylaldehyde (0.381 g, 98%). Anal. Calcd for $C_{17}H_{15}N_3O_4Cu$ (388.87): C, 52.51; H, 3.89; N, 10.81. Found: C, 52.29; H, 3.88; N, 11.10. IR (KBr): 1619 ($\nu_{C=N}$), 1309 (ν_{NO_2}) cm^{-1}. FAB-MS: m/z 389 [M + H$^+$].

1n. From **IN4** and 5-methylsalicylaldehyde (0.400 g, 95%). Anal. Calcd for $C_{18}H_{17}N_3O_4Cu\cdot H_2O$ (420.91): C, 51.36; H, 4.55; N, 9.98. Found: C, 51.33; H, 4.15; N, 9.74. IR (KBr): 1628 ($\nu_{C=N}$), 1312 (ν_{NO_2}) cm^{-1}. FAB-MS: m/z 403 [M + H$^+$].

1o. From **IN4** and 5-methoxysalicylaldehyde (0.406 g, 92%). Anal. Calcd for $C_{18}H_{17}N_3O_5Cu\cdot{}^5/_4H_2O$ (441.42): C, 48.98; H, 4.45; N, 9.52. Found: C, 49.00; H, 4.26; N, 9.51. IR (KBr): 1627 ($\nu_{C=N}$), 1308 (ν_{NO_2}) cm^{-1}. FAB-MS: m/z 419 [M + H$^+$].

1p. From **IN4** and 5-(dimethylamino)salicylaldehyde (0.397 g, 92%). Anal. Calcd for $C_{19}H_{20}N_4O_4Cu$ (431.94): C, 52.83; H, 4.67; N, 12.97. Found: C, 52.63; H, 4.56; N, 12.66. IR (KBr): 1627 ($\nu_{C=N}$), 1309 (ν_{NO_2}) cm^{-1}. FAB-MS: m/z 431 [M$^+$].

X-ray Crystal Structure Determinations. Details of the procedures concerning data collection and structure refinement are reported in Table 1. Crystals were mounted on a glass fiber in a random orientation and collected at room temperature on a Siemens SMART CCD area detector diffractometer. Graphite-monochromatized Mo Kα radiation (λ = 0.710 73 Å) was used with the generator working at 45 kV and 40 mA. Preliminary cell parameters and orientation matrices were obtained from least-squares refinement on reflections measured in three different sets of 20 frames each, in the range $0 < \theta < 25°$. Intensity data were collected in the full sphere (ω-scan method), 2100 frames (20 s per frame; $\Delta\omega$ = 0.3°), and the first 100 frames were re-collected to monitor the crystal decay, which was not observed in all cases. An absorption correction was applied using the *SADABS* routine.[14] The structures were solved by direct methods using *SHELXS 86*,[15] and full-matrix least-squares refinements on F^2 were performed using the *SHELXL 97* program,[16] implemented in the *WINGX* suite.[17] All non-H atoms were refined anisotropically, and the H atoms were included in the structure model riding on their C atom.

Crystallographic data (excluding structure factors) for the structures reported in this paper have been deposited with the Cambridge Crystallographic Data Centre as supplementary publication nos. CCDC 608121−608124. Copies of the data can be obtained free of charge on application to The Director, CCDC, 12 Union Road, Cambridge CB2 1EZ, U.K. (fax int. code + (1223) 336-033; e-mail teched@chemcrys.cam.ac.uk).

EFISH Measurements. The molecular NLO responses were measured by the solution-phase direct-current electric-field-induced second-harmonic (EFISH) generation method,[18] which provides γ_{EFISH}, that is, the direct information on the molecular NLO properties, through

$$\gamma_{EFISH} = (\mu\beta_\lambda/5kT) + \gamma(-2\omega;\omega,\omega,0)$$

where $\mu\beta_\lambda/5kT$ is the dipolar orientational contribution, λ is the fundamental wavelength of the incident photon in the EFISH experiment, $\gamma(-2\omega;\omega,\omega,0)$, a third-order term at frequency ω of the incident light, is the cubic electronic contribution to γ_{EFISH}, which is negligible for the kinds of molecules investigated here,[3a,b] and β_λ is the projection along the dipole moment axis of the vectorial component, hereafter called β_{vec}, of the quadratic hyperpolarizability tensor. EFISH measurements were carried out in our department in $CHCl_3$ solutions working at a nonresonant incident wavelength of 1.907 μm, using a Q-switched, mode-locked Nd3+:YAG laser, manufactured by Atalaser, equipped with a Raman

(14) Sheldrick, G. M. *SADABS, Area-Detector Absorption Correction Program*; Bruker AXS, Inc.: Madison, WI, 2000.
(15) Sheldrick, G. M. *SHELXS 86. Acta Crystallogr., Sect A* **1990**, *46*, 467−473.
(16) Sheldrick, G. M. *SHELXL 97, Program for Crystal Structure Refinement*; University of Göttingen: Göttingen, Germany, 1997.
(17) Farrugia, L. J. *J. Appl. Crystallogr.* **1999**, *32*, 837−838.
(18) (a) Levine, B. F.; Bethea, C. G. *Appl. Phys. Lett.* **1974**, *24*, 445−447. (b) Singer, K. D.; Garito, A. F. *J. Chem. Phys.* **1981**, *75*, 3572−3580. (c) Ledoux, I.; Zyss, J. *Chem. Phys.* **1982**, *73*, 203−213.

shifter; the apparatus for the EFISH measurements was made by SOPRA (Dijon, France).

Solvatochromism. UV−visible spectra were recorded with a Jasco V-530 spectrophotometer; λ values are accurate to ±0.5 nm. Absorption spectra of compounds **1** follow the Lambert−Beer law in the 5×10^{-4}−5×10^{-6} mol L^{-1} range. Spectra deconvolutions were performed by means of Microcal Origin (version 6.0), using Gaussian functions.

The CT contribution to hyperpolarizability, β_{CT}, was determined according to Oudar and Chemla's "two-state" model:[19]

$$\beta_{CT} = \frac{3}{2}\frac{\Delta E_{eg}{}^2 \mu_{eg}{}^2 \Delta\mu_{eg}}{(\Delta E_{eg}{}^2 - E_L{}^2)(\Delta E_{eg}{}^2 - 4E_L{}^2)}$$

where ΔE_{eg} is the transition energy, μ_{eg} is the transition dipole moment, $\Delta\mu_{eg}$ is the dipole moment variation between the ground and excited states, and E_L is the energy of the laser used for EFISH measurements (1.907 μm, 5244 cm^{-1}). It is also possible to isolate the $\beta_{0,static}$ value from the dependence on E_L, reprocessing the former equation in the following formula:[6a,20]

$$\beta_{CT} = \beta_{0,static}F(\omega) = \frac{3\mu_{eg}{}^2\Delta\mu_{eg}}{2\Delta E_{eg}{}^2}\frac{\Delta E_{eg}{}^4}{(\Delta E_{eg}{}^2 - E_L{}^2)(\Delta E_{eg}{}^2 - 4E_L{}^2)}$$

where the second term is the dispersion factor $F(\omega)$. The quantities occurring in the expression of β_{CT} have been determined by spectroscopic measurements.

The transition dipole moment, μ_{eg}, was evaluated by the relationship[5a,21]

$$\mu_{eg}{}^2 = \frac{3\ln\epsilon_0 ch}{2\pi\omega_{eg}N_A}\frac{n}{f^2}\int\epsilon(\omega)\,d\omega$$

where ϵ_0 is the vacuum permittivity, c is the speed of light in the vacuum, h is Planck's constant, ω_{eg} is the transition frequency (s^{-1}) in the solvent, and N_A is Avogadro's number. The reported integral is the area of the absorption band (m^2 mol^{-1} s^{-1}), and $n/f^2 = 9n/(n^2 + 2)^2$ (n being the refractive index of the solvent) is the correction factor accounting for the influence of the medium.

The oscillator strength, f, of the associated absorption band was evaluated from the transition dipole moment, μ_{eg}, by the relationship

$$f = \frac{2m\omega_{eg}}{e^2\hbar}\mu_{eg}{}^2 = \frac{3\ln\epsilon_0 c(2m)}{N_A e^2}\frac{n}{f^2}\int\epsilon(\omega)\,d\omega$$

where m is the mass of the electron.

The dipole moment variation between the ground and excited states, $\Delta\mu_{eg}$, was determined from the solvatochromism of the relevant absorption bands by means of the McRae equation,[22] which, supposing dispersive interactions to be negligible, reduces to

$$\nu_s = \nu_g + A\left(\frac{n^2-1}{2n^2+1}\right) + B\left(\frac{\epsilon-1}{\epsilon+2} - \frac{n^2-1}{n^2+2}\right)$$

where ν_s and ν_g are the frequencies (cm^{-1}) of the absorption maximum in a given solvent and in the gaseous phase, respectively, ϵ is the solvent dielectric constant, and the constants A and B are

$$A = -\frac{\mu_e{}^2 - \mu_g{}^2}{hca^3}, \quad B = -\frac{2\mu_g\Delta\mu_{eg}}{hca^3}$$

where a is the Onsager radius, estimated as 0.7 times the maximum length of the molecule. Determination of $\Delta\mu_{eg}$ was performed by measurements of the absorption frequencies in different solvents, according to the reprocessing methodology suggested in the literature.[23]

Computational Details. The molecular geometries of all complexes have been fully optimized at the restricted open-shell (RO) B3LYP/6-311++G** level using the *Gaussian03* package.[24] The RO wave function was required by the presence of the d^9 open-shell Cu(II) atom. The optimized structures of the unsubstituted complexes **1a** and **1i** have been used as starting geometries for the other complexes, by appropriately adding the electron donor and/or acceptor substituents. For the en complexes (**1b**−**1h**), the same optimized geometries were expected independently on the opposite side to where the substitutions were made, owing to the symmetry of **1a**. On the other hand, the tn derivative **1i** was found intrinsically asymmetric, and this made it possible to have two different geometries for each complex of the series **1j**−**1p**, according to two possible schemes of substitution. In each case, both structures have been submitted to geometry optimization. The corresponding Cu−O and Cu−N bond lengths were found to differ by as much as 0.028 Å, while the associated energies differ by less than 0.1 kcal mol^{-1}.

The static first hyperpolarizabilities have been calculated at the ROB3LYP/6-311++G** level using the finite-field method. The strength of the electric field to be applied has been tested by systematically varying the step size from 0.003 to 0.0001 au and checking the convergence in the most significant β_{ijk} components of the hyperpolarizability tensor. The default value (0.001 au) was found to be suitable for evaluating these quantities. For the tn complexes, β_{ijk} calculations were performed on only one of the two minimum structures (the "down" isomer; see below). The Taylor series convention AB for reporting the β_{ijk} values will be used.[25]

Electronic absorption spectra of selected complexes in the previously optimized geometries were computed using the spin-unrestricted TDDFT approach as implemented in the RESPONSE module of the Amsterdam Density Functional program (ADF version 2005.01).[26] For the exchange-correlation functional, we employed the generalized gradient approximated correction by

(19) Oudar, J. L.; Chemla, D. S. *J. Chem. Phys.* **1977**, *66*, 2664−2668.
(20) Di Bella, S. *New J. Chem.* **2002**, *26*, 495−497.
(21) (a) Bosshard, C.; Knopfle, G.; Pretre, P.; Gunter, P. *J. Appl. Phys.* **1992**, *71*, 1594−1605. (b) Paley, M. S.; Harris, J. M. *J. Org. Chem.* **1989**, *54*, 3774−3778.
(22) McRae, E. G. *J. Phys. Chem.* **1957**, *61*, 562−572.
(23) Bruni, S.; Cariati, E.; Cariati, F.; Porta, F. A.; Quici, S.; Roberto, D. *Spectrochim. Acta, Part A* **2001**, *57*, 1417−1426.
(24) Frisch, M. J.; Trucks, G. W.; Schlegel, H. B.; Scuseria, G. E.; Robb, M. A.; Cheeseman, J. R.; Montgomery, J. A., Jr.; Vreven, T.; Kudin, K. N.; Burant, J. C.; Millam, J. M.; Iyengar, S. S.; Tomasi, J.; Barone, V.; Mennucci, B.; Cossi, M.; Scalmani, G.; Rega, N.; Petersson, G. A.; Nakatsuji, H.; Hada, M.; Ehara, M.; Toyota, K.; Fukuda, R.; Hasegawa, J.; Ishida, M.; Nakajima, T.; Honda, Y.; Kitao, O.; Nakai, H.; Klene, M.; Li, X.; Knox, J. E.; Hratchian, H. P.; Cross, J. B.; Adamo, C.; Jaramillo, J.; Gomperts, R.; Stratmann, R. E.; Yazyev, O.; Austin, A. J.; Cammi, R.; Pomelli, C.; Ochterski, J. W.; Ayala, P. Y.; Morokuma, K.; Voth, G. A.; Salvador, P.; Dannenberg, J. J.; Zakrzewski, V. G.; Dapprich, S.; Daniels, A. D.; Strain, M. C.; Farkas, O.; Malick, D. K.; Rabuck, A. D.; Raghavachari, K.; Foresman, J. B.; Ortiz, J. V.; Cui, Q.; Baboul, A. G.; Clifford, S.; Cioslowski, J.; Stefanov, B. B.; Liu, G.; Liashenko, A.; Piskorz, P.; Komaromi, I.; Martin, R. L.; Fox, D. J.; Keith, T.; Al-Laham, M. A.; Peng, C. Y.; Nanayakkara, A.; Challacombe, M.; Gill, P. M. W.; Johnson, B.; Chen, W.; Wong, M. W.; Gonzalez, C.; Pople, J. A. *Gaussian 03*, revision B.04; Gaussian, Inc.: Pittsburgh, PA, 2003.
(25) Willets, A.; Rice, J. E.; Burlad, D. M.; Shelton, D. P. *J. Chem. Phys.* **1992**, *97*, 5790−5799.
(26) te Velde, G.; Bickelhaupt, F. M.; van Gisbergen, S. J. A.; Fonseca Guerra, C.; Baerends, E. J.; Snijders, J. G.; Ziegler, T. *J. Comput. Chem.* **2001**, *22*, 931−967.

Scheme 1. Synthetic Procedure

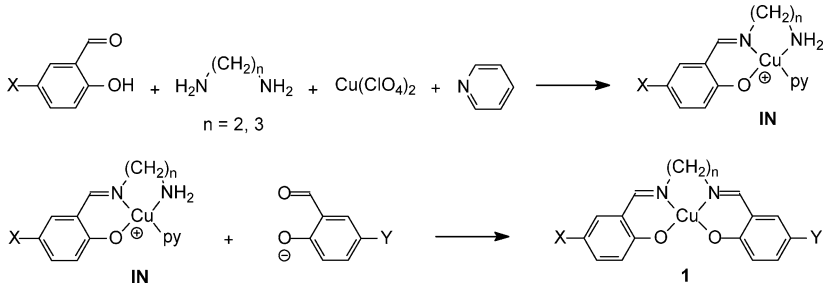

Becke[27] and Lee−Yang−Parr[28] (BLYP). Test calculations were also performed with the van Leeuwen−Baerends (LB94) exchange-correlation potential,[29,30] which corrects the local density approximation (LDA) potential in the outer region of the molecule. However, in this case, the excitation energies were found to be largely shifted downward (by more than 3000 cm^{-1}) with respect to the experimental values, as was already observed in other transition-metal compounds.[31] Owing to the spectral range examined here, where only low-lying single excitations are considered, we deemed it appropriate to use the adiabatic LDA for the exchange-correlation kernel, in which the frequency dependence of the kernel is ignored.[31] Calculations were performed with the ADF triple-ζ doubly polarized Slater-type orbital basis set "TZ2P" for all atoms, with a 1s frozen core for C, N, and O atoms and up to a 2p frozen core for Cu. The use of a more extended basis set, such as the quadruple-ζ quality diffuse even-tempered "ET-pVQZ" basis set, on a selected compound (**1h**) was not found to modify the transition energies and the oscillator strengths in a significant way.

Solvent effects were evaluated using the conductor-like screening model (COSMO) as implemented in ADF,[32] using Bondi's van der Waals atomic radii to build the cavity around each atom. The introduction of solvent effects in the calculations determined a blue shift of the more significant transitions of 1200−1900 cm^{-1} and an increase of the oscillator strength with respect to the isolated molecule.

Results and Discussion

Synthesis and Characterization. The synthesis of the unsymmetrically substituted salen analogues must proceed in two steps, i.e., monocondensation of 1 mol of a salicylaldehyde with a diamine to give "half-unit" intermediates, which are then allowed to react with another salycilaldehyde. A survey of the literature has shown that some "half-unit" intermediates can be synthesized from salicylaldehyde and certain diamines, such as *o*-phenylenediamine or 1,2-diaminocyclohexane.[33] However, with ethylenediamine or 1,3-diaminopropane, we were unable to obtain such monocondensation products: reaction of equimolar amounts of salicylaldehyde and these diamines gave invariably the double-condensation products H_2salen or H_2saltn, respectively, which were obtained even when a 4-fold excess of the diamine was used. A general preparation strategy, independent of the nature of the diamine, is outlined in Scheme 1. Following Costes et al.,[12] the monocondensation "half-unit" Schiff bases can be obtained, as their copper(II) complexes, by a template synthesis upon reaction of a salicylaldehyde, a diamine, and copper perchlorate, or nitrate, in a 1:1:1 ratio. Because these "half-units" are tridentate ligands, tetracoordination of Cu(II) is achieved through the formation of phenolato-bridged bi- or polynuclear species;[34] however, if the reaction is carried out in the presence of a slight excess of pyridine, the mononuclear compounds **IN** are obtained in good yields. To synthesize compounds **1b**−**1h** and **1j**−**1p**, we have prepared the four intermediates depicted in Chart 1, with en or tn and X = H or NO_2; the reaction of these intermediates with the sodium salt of a different salicylaldehyde (Y = H, Me, OMe, NMe_2) gave the push−pull derivatives in high to moderate yields. All compounds were characterized by elemental analyses and FAB-MS.

X-ray Structures of Compounds 1g, 1n, 1o, and 1p. Crystals suitable for X-ray diffraction studies were obtained by slow diffusion of ethyl acetate into a dimethyl sulfoxide (DMSO) solution (**1g**) or diisopropyl ether into $CHCl_3$ solutions (**1n**, **1o**, and **1p**). Relevant bond lengths and angles are reported in Table 2, while the structures of **1g**, **1n**, and **1p** are presented in Figures 1−4. The four compounds crystallize in stacked couples in a head-to-tail fashion, i.e., with the electron-withdrawing side above the electron-releasing one.

Molecules of compound **1g** are packed in the crystal to form centrosymmetric pairs with the nitro group stacked almost above the moiety bearing the electron donor substituent (see Figure 1). The Cu···O1($-x,-y,-z-1$) interaction of 3.55 Å is about 1 Å larger than a typical Cu−O distance corresponding to an apical position for a square-pyramidal-coordinated Cu ion.[35,36] Atoms C8 and C9 are significantly out of the plane, as can be appreciated from the torsion angle N1−C8−C9−N2, which is −36.6(5)°. The

(27) Becke, A. D. *Phys. Rev. A* **1988**, *38*, 3098−3100.
(28) Lee, C.; Yang, W.; Parr, R. G. *Phys. Rev. B* **1988**, *37*, 785−789.
(29) van Leeuwen, R.; Baerends, E. J. *Phys. Rev. A* **1994**, *49*, 2421−2431.
(30) van Gisbergen, S. J. A.; Snijders, J. G.; Baerends, E. J. *J. Chem. Phys.* **1998**, *109*, 10657−10658.
(31) van Gisbergen, S. J. A.; Groeneveld, J. A.; Rosa, A.; Snijders, J. G.; Baerends, E. J. *J. Phys. Chem. A* **1999**, *103*, 6835−6844.
(32) Pye, C. C.; Ziegler, T. *Theor. Chem. Acc.* **1999**, *101*, 396−408.
(33) (a) Lopez, J.; Liang, S.; Bu, X. R. *Tetrahedron Lett.* **1998**, *39*, 4199−4202. (b) Lopez, J.; Mintz, E. A.; Hsu, F.-L.; Bu, X. R. *Tetrahedron Asymm.* **1998**, *9*, 3741−3744. (c) Dalla Cort, A.; Mandolini, L.; Palmieri, G.; Pasquini, G.; Schiaffino, L. *Chem. Commun.* **2003**, 2178−2179. (d) Kleij, A. W.; Tooke, D. M.; Spek, A. L.; Reek, J. N. H. *Eur. J. Inorg. Chem.* **2005**, 4626−4634.
(34) (a) Leluk, M.; Jezowska-Trzebiatowska, B. *Polyhedron* **1991**, *10*, 1053−1056. (b) Costes, J. P. *Bull. Soc. Chim. Fr.* **1986**, 78−82. (c) Mandal, S. K.; Nag, K. *J. Chem. Soc., Dalton Trans.* **1984**, 2839−2841.
(35) Nathan, L. C.; Koehne, J. E.; Gilmore, J. M.; Hannibal, K. A.; Dewhirst, W. E.; Mai, T. D. *Polyhedron* **2003**, *23*, 887−894.
(36) Bhadbhade, M. M.; Srinivas, D. *Inorg. Chem.* **1993**, *32*, 6122−6130.

Table 2. Coordination Bond Lengths (Å) and Angles (deg) of Compounds **1g**, **1n**, **1o**, and **1p**[a]

		1n			
	1g	molecule a	molecule b	**1o**	**1p**
Cu−O1	1.923(3)	1.934(2)	1.937(2)	1.942(5)	1.940(5)
Cu−O2	1.898(2)	1.948(2)	1.936(2)	1.909(5)	1.912(6)
Cu−N1	1.942(3)	2.016(2)	1.999(2)	1.961(7)	1.978(7)
Cu−N2	1.934(3)	1.969(2)	1.987(2)	1.966(6)	1.971(7)
O1−Cu−O2	91.2(1)	83.23(8)	82.08(8)	82.7(2)	82.3(2)
N1−Cu−N2	83.5(1)	95.23(10)	96.98(9)	94.2(3)	94.6(3)
O1−Cu−N1	92.5(1)	91.07(9)	91.27(8)	90.6(3)	91.3(2)
O2−Cu−N2	93.4(1)	90.15(9)	90.98(9)	92.5(2)	91.6(3)
O−N···N−O dihedral angle	−8.0(9)	−2.8(8)	13.0(8)	1.1(15)	−4.0(20)

[a] Atoms "1" refer to the salicylaldehyde moiety bearing the NO_2 group.

coordination plane including the Cu atom and the donor atoms of the Schiff base is essentially planar, with a maximum deviation from the mean plane of 0.10 Å for atom N1.

The asymmetric unit of compound **1n** contains two independent molecules of the complex (molecules a and b) and a water molecule. The latter is H-bonded to the nitro group of molecule a [O(W)···O3a = 3.161(5) Å] and to the phenolato O atoms of molecule b [O(W)···O1b = 3.103(5) Å; O(W)···O2b = 3.095(5) Å] (see Figure 2). Each of the two independent molecules of the complex interacts with an adjacent molecule, related by a center of symmetry, to form pairs similar to those observed for compound **1g** (see Figure 3). In this case, the distance between the Cu ion and a phenolato O atom of the adjacent molecule is shorter than that in the case of **1g** and consistent with a square-pyramidal-coordinated Cu ion [Cua···O2a($-x$,1$-y$,2$-z$) = 2.463(3) Å and Cub···O2b($-x$,1$-y$,1$-z$) = 2.569(3) Å]. Pairs of centrosymmetric molecules are stacked in the crystal on parallel planes with a weak interaction between molecules of type a and molecules of type b [Cub···O1a($-x$,1$-y$,2$-z$) = 3.570(2) Å]. The six-membered diamine chelate rings display a distorted half-chair conformation.

Compounds **1o** and **1p** contain a chloroform molecule H-bonded to the phenolato O atoms of the complex. In the crystal, each complex molecule interacts with an adjacent centrosymmetric molecule to form stacked pairs similar to those observed for compounds **1g** and **1n** (see Figure 4). However, the packing is slightly different because in **1o** the distance between the Cu ion and the phenolato O atom of the centrosymmetrically related molecule Cu···O1 is 2.905(6) Å, whereas in **1p** the interaction is with O2 and is shorter, 2.690(6) Å. Such a difference can be hardly attributed to electronic effects because in both complexes the Cu−O and Cu−N distances are essentially identical. Probably steric effects, related to the different orientations of the chloroform molecule and its contacts with the phenolato O atoms, can account for the difference.

A point of interest of these complexes is the relative influence of the D and A groups on the Cu−O and Cu−N coordination bonds. This can be appreciated in complexes **1g**, **1o**, and **1p** because in **1n** coordination bonds lengths are perturbed by intermolecular interactions. In the former compounds, where these interactions are weak, we observe a significant difference in the Cu−O bond lengths, about 0.02−0.03 Å longer for the *p*-nitrosalicylaldimino moiety. The Cu−N distances are less affected.

Geometry Optimizations. To investigate in more detail the influence of the A and D groups on the Cu−O and Cu−N coordination bonds, we have undertaken a DFT theoretical investigation, optimizing the geometry of all complexes at the ROB3LYB/6311++G** level of computation.[24]

All optimized geometries present a tetrahedral distortion around Cu, larger in the tn derivatives (O−N···N−O dihedral angle of around 25°) than in the en compounds (10°), in agreement with most of the reported crystal structures of [Cu(salen)] and [Cu(saltn)][35,37,38] [in the X-ray structures of **1g** and **1n**−**1p**, coordination around Cu is more planar (Table 2) presumably as a result of the observed stacking interactions]. The relevant geometric parameters are listed in Table 3. The coordination bonds (in particular Cu−N) ended up being slightly longer than those found in crystal structures,[35−38] but these differences are of the same order of magnitude by which experimental metal−ligand bond lengths are generally reproduced by gradient-corrected DFT methods.[9a]

The data of Table 3 show that the effect of the D groups on the coordination bond lengths is vanishingly small (compounds **1b**−**1d**); on the contrary, the presence of NO_2 on one sal moiety (compound **1e**, A = NO_2, D = H) causes an elongation of Cu−O(A), with a concomitant decrease of Cu−O(D), compared to **1a** (+0.015 and −0.012 Å, respectively; O(A) and O(D) are the phenolato O atoms of the sal moieties with the acceptor and donor groups). The presence of NO_2 influences also the Cu−N bonds, although to a lesser extent: a slight elongation of Cu−N(A) and a slight shortening of Cu−N(D) (both about 0.010 Å). The introduction of donor groups on the other (unsubstituted) sal of **1e** gives rise to the push−pull compounds **1f**−**1h**. Again, the D groups have little influence on the coordination bonds, which are very similar to those of **1e**. In conclusion, our results suggest that only NO_2 is able to influence the coordination bonds in these molecules in an appreciable way.

The optimized geometry of [Cu(saltn)] (**1i**) was not found to be symmetrical, in the sense that the two Cu−O bonds and, particularly, the two Cu−N bonds differ by 0.006 and 0.025 Å, respectively. Although this result may at first sight seem odd, it must be noted that, in the reported crystal structures of this compound, the two Cu−O and the two Cu−N coordination bonds are as different as 0.02 and 0.03 Å, respectively.[35,37−39] As to the origin of this unequivalence, we think it arises from the presence of three fused six-membered rings; in particular, the diamine chelate ring of tn is out of the coordination pseudoplane (see Figures 2−4), but it can be neither gauche, as in the en case, nor in a "relaxed" chair conformation like that of cyclohexane, both

(37) Xiong, R.-G.; Song, B.-L.; Zuo, J.-L.; You, X.-Z. *Polyhedron* **1996**, *15*, 903−907.
(38) Hasegawa, M.; Kumagai, K.-i.; Terauchi, M.; Nakao, A.; Okubo, J.; Hoshi, T. *Monatsh. Chem.* **2002**, *133*, 285−298.
(39) Drew, M. G. B.; Prasad, R. N.; Sharma, R. P. *Acta Crystallogr., Sect. C* **1985**, *C41*, 1755−1758.

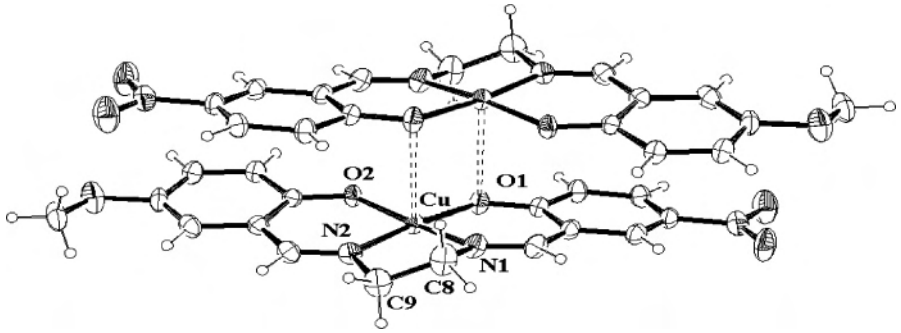

Figure 1. Pair of centrosymmetric molecules of compound **1g**.

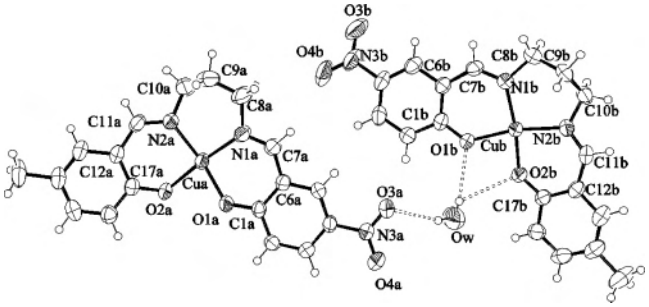

Figure 2. Asymmetric unit of compound **1n**.

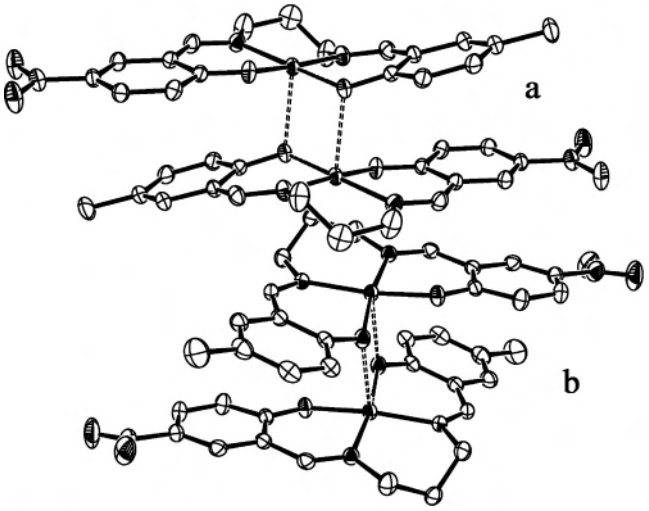

Figure 3. Stacking of centrosymmetric pairs of molecules a and b in compound **1n**.

because the N−Cu−N angle must be close to 90° and because of the trigonal geometry of the N atoms of the azomethine groups. Our results suggest that the stress arising from such requirements is relaxed by (i) a widening of the N−Cu−N angles, with concomitant narrowing of the O−Cu−O angles, compared to en derivatives, (ii) a tetrahedral distortion of the CuN_2O_2 coordination set larger than that of the en complexes, and (iii) the unequivalence of the Cu−N bonds.

If we now want to build and optimize the unsymmetrically substituted compounds **1j**−**1p** from **1i**, a problem arises: on which side shall we put the various A and D substituents? We have, in fact, considered both possibilities by generating and optimizing two different isomers, presented in Table 3.

Because the tn chain can be on either side of the coordination pseudoplane, we need a convention to describe

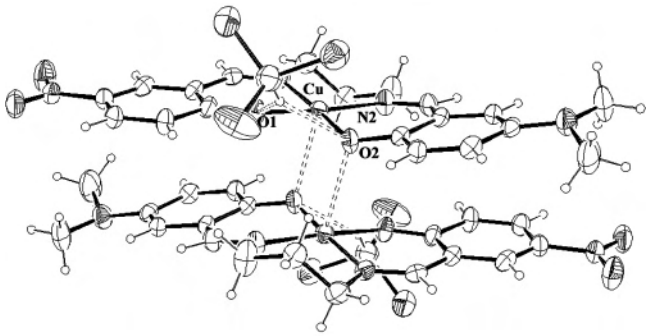

Figure 4. Pair of centrosymmetric molecules of compound **1p**, interacting with the chloroform molecules.

the geometry of these derivatives. This is illustrated in Figure 5, where the molecules are viewed along the *y* axis, from the side of the phenolato O atoms and with the electron acceptor group on the left-hand side. We shall use the descriptors "down" and "up" according to the position of the trimethylene chain with respect to the coordination pseudoplane. It must be noted that, because of this convention, when we build **1j**−**1p** from **1i**, putting a substituent on the sal moiety with the short, rather than the long Cu−N distance, will result in an inversion of the down and up conformation of tn, as illustrated in Figure 5. Finally, we started to build these molecules from **1i** with the Λ configuration around Cu, and, consequently, **1j**−**1p** have this configuration. Each down or up isomer has its Δ enantiomer (Figure 5), which has the same energy; the results of Table 3 are therefore comprehensive.

The presence, in the down isomer, of the A substituent on the sal moiety with the long Cu−N distance and of the D substituent on the sal moiety with the short Cu−N distance, increases the difference between these two coordination bonds, whereas putting the A and D groups the other way around (i.e., in the up isomer) has the effect of decreasing such a difference. Also in the tn derivatives, the major effect on the coordination bonds is given by NO_2, with elongations and contractions similar to the en case. Interestingly, the amounts of computed elongations and contractions of the coordination bonds are similar to those found in the crystal structures of compounds **1g**, **1o**, and **1p**.

Dipole Moments. A further interest of our compounds is the deviation of μ_g from the direction along the *y* axis (the intrinsic direction in the parent [Cu(salen)]) due to a component of the dipole moment along the *x* axis originated by the charge asymmetry. In Table 4, we report the calculated

Table 3. Coordination Bonds (Å) and Angles (deg) of the Optimized Geometries[a]

compd	A, D, diamine	Cu−O(A)	Cu−O(D)	Cu−N(A)	Cu−N(D)	O−Cu−O	N−Cu−N
1a	H, H, en	1.926	1.925	1.976	1.976	93.25	83.65
1b	H, Me, en	1.927	1.925	1.977	1.975	93.18	83.65
1c	H, OMe, en	1.929	1.920	1.977	1.977	93.29	83.63
1d	H, NMe_2, en	1.928	1.924	1.978	1.973	93.25	83.66
1e	NO_2, H, en	1.941	1.914	1.983	1.967	92.93	83.79
1f	NO_2, Me, en	1.942	1.913	1.983	1.966	92.97	83.79
1g	NO_2, OMe, en	1.943	1.908	1.984	1.969	93.02	83.73
1h	NO_2, NMe_2, en	1.943	1.911	1.985	1.965	93.01	83.78
1i	H, H, tn	1.930	1.936	2.025	2.000	86.24	97.38
1j	H, Me, tn	1.931[d]	1.935[d]	2.024[d]	1.998[d]	86.50[d]	97.43[d]
		1.937[u]	1.929[u]	2.001[u]	2.023[u]	86.24[u]	97.38[u]
1k	H, OMe, tn	1.933[d]	1.929[d]	2.023[d]	2.001[d]	86.82[d]	97.46[d]
		1.938[u]	1.925[u]	2.001[u]	2.027[u]	86.56[u]	97.33[u]
1l	H, NMe_2, tn	1.933[d]	1.933[d]	2.024[d]	1.997[d]	86.59[d]	97.51[d]
		1.939[u]	1.926[u]	2.001[u]	2.026[u]	86.43[u]	97.34[u]
1m	NO_2, H, tn	1.946[d]	1.924[d]	2.033[d]	1.993[d]	85.42[d]	97.48[d]
		1.952[u]	1.919[u]	2.008[u]	2.014[u]	85.73[u]	97.61[u]
1n	NO_2, Me, tn	1.948[d]	1.923[d]	2.034[d]	1.992[d]	85.47[d]	97.47[d]
		1.954[u]	1.918[u]	2.008[u]	2.013[u]	85.78[u]	97.58[u]
1o	NO_2, OMe, tn	1.949[d]	1.918[d]	2.033[d]	1.994[d]	85.90[d]	97.52[d]
		1.955[u]	1.913[u]	2.009[u]	2.019[u]	86.07[u]	97.52[u]
1p	NO_2, NMe_2, tn	1.949[d]	1.922[d]	2.035[d]	1.990[d]	85.62[d]	97.52[d]
		1.955[u]	1.916[u]	2.009[u]	2.011[u]	85.97[u]	97.70[u]

[a] O(A), O(D), N(A), and N(D) refer to the phenolato O atoms and the imino N atoms of the sal moieties bearing the electron acceptor (A) and donor (D) groups. The superscripts d and u refer to the "down" and "up" conformations of the chelate ring of tn; see text.

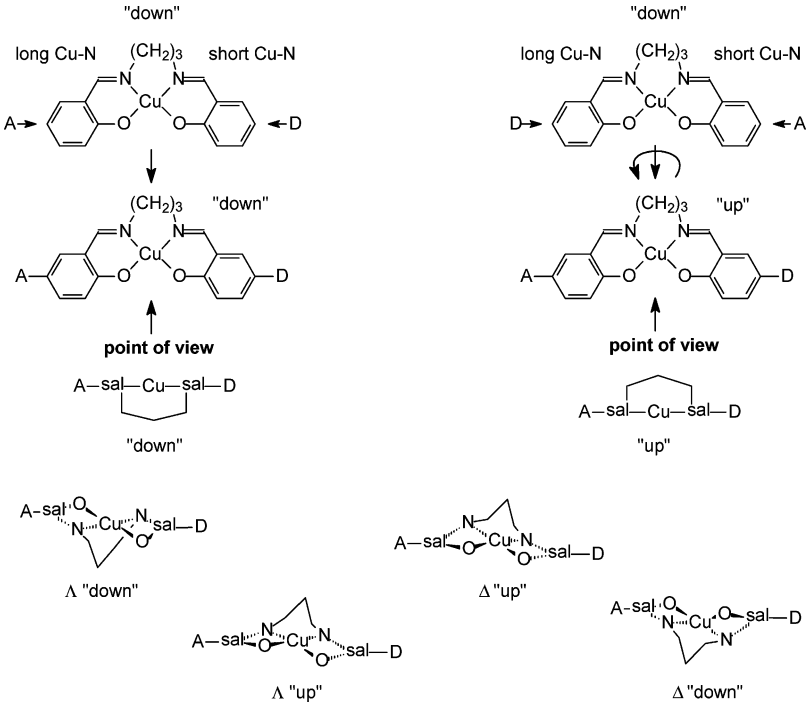

Figure 5. "Down" and "up conventions.

ground-state dipole moments μ_g of all compounds, their components, and the angle ϕ between μ_g and the *y* axis (see two examples in Figure 6). The reliability of our computations is given by the agreement between the calculated and experimental μ_g values (measured by the Guggenheim method[11]) of some selected compounds, also reported in Table 4.

The presence of A and/or D in position 5 of sal affects only marginally μ_y. The slight decrease of μ_y in complexes with OMe is due to the fact that we optimized the geometry with the methyl group pointing toward the negative *y* direction. As expected, both A and D substituents generate an *x* component; interestingly, however, our results show that only the electron acceptor (NO_2) group produces a relevant μ_x value (compare, for instance, **1a**−**1d** with **1e**), which causes a substantial deviation of μ_g from the *y* axis (large ϕ values). The electron donor groups have only a minor influence on ϕ, with the highest being given by NMe_2. The low, but significant, μ_z (i.e., a component perpendicular to the pseudoplane of the molecule) of the tn derivatives is a consequence of the large distortion from planarity of these compounds (see above).

Electronic Spectra. The electronic spectra of compounds **1** (see two examples in Figure 7) consist of d−d bands in

Table 4. Experimental ($CHCl_3$ Solutions) and Computed Dipole Moments (Debye)[a]

compd	A, D, diamine	$\mu_{g,exptl}$	$\mu_{g,calcd}$	μ_x	μ_y	μ_z	ϕ (deg)
1a	H, H, en	5.8 ± 0.4	6.12	0.00	6.12	−0.01	0.0
1b	H, Me, en	5.8 ± 0.5	5.98	0.39	5.97	−0.02	3.5
1c	H, OMe, en		4.89	0.31	4.88	−0.14	3.7
1d	H, NMe_2, en		6.17	1.05	6.05	−0.60	11.3
1e	NO_2, H, en	9.2 ± 1.5	9.77	7.69	6.02	−0.01	51.9
1f	NO_2, Me, en		10.12	8.15	6.01	−0.02	53.6
1g	NO_2, OMe, en		9.60	8.08	5.17	−0.14	57.4
1h	NO_2, NMe_2, en		10.87	8.93	6.16	−0.57	55.5
1i	H, H, tn		5.89	0.10	5.87	−0.42	4.7
1j	H, Me, tn		5.69	0.25	5.67	−0.44	4.8
1k	H, OMe, tn		4.61	0.08	4.58	0.54	6.5
1l	H, NMe_2, tn		5.65	0.65	5.60	0.22	7.6
1m	NO_2, H, tn	10.1 ± 0.9	10.32	8.11	6.37	0.42	51.8
1n	NO_2, Me, tn		10.57	8.28	6.56	0.36	51.6
1o	NO_2, OMe, tn	9.8 ± 1.5	9.86	7.85	5.96	0.24	52.8
1p	NO_2, NMe_2, tn	10.6 ± 0.8	11.17	8.73	6.97	−0.21	51.4

[a] The computed μ_g values of the tn derivatives are those of the "down" isomers; those of the "up" isomers differ by less than 1%.

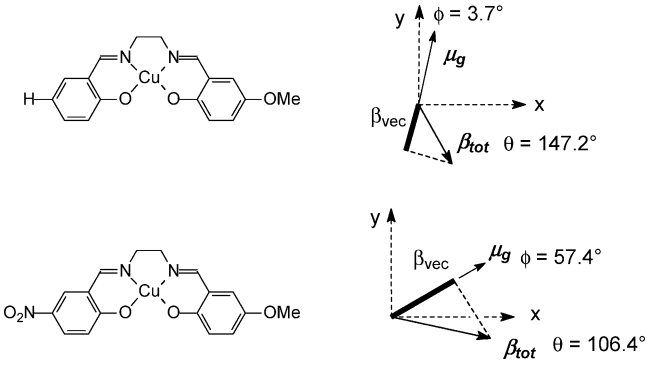

Figure 6. Definitions of the angles ϕ and θ and projection of β_{tot} along μ_g.

the 15 000−20 000-cm^{-1} range, with ϵ 100−400 L mol^{-1} cm^{-1}, and a broad absorption, in the near-UV region (20 000−33 000 cm^{-1}), with an irregular shape and a shoulder at lower wavenumbers. Deconvolution of this absorption has shown the presence of three bands (see Table 5 and two examples in Figure 8), which, in the case of **1a** ($CHCl_3$ solution), are at 25 262 cm^{-1} ($\epsilon \sim 10^3$ L mol^{-1} cm^{-1}), 27 201 cm^{-1} ($\epsilon \sim$ 8000 L mol^{-1} cm^{-1}), and 27 228 cm^{-1} ($\epsilon \sim$ 2700 L mol^{-1} cm^{-1}). In some cases, we were unable to find the three components, particularly the position of the first band. Following literature data,[40,41] the first band is attributed to a CT transition, while the other two are attributed to intraligand $\pi-\pi^*$ transitions, essentially involving the azomethine groups.

The CT band is strongly influenced by the presence of D groups, which produce a bathochromic shift, particularly relevant in the case of **1d** (A = H; D = NMe_2), whereas the presence of the nitro group gives rise to a slight hypsochromic shift (Table 5). These behaviors suggest a ligand-to-metal CT (LMCT) nature of this transition. The compounds with the nitro group show also a rather intense ($\epsilon \sim$ 20 000 L mol^{-1} cm^{-1}) component in the high-energy part of the broad absorption.

(40) Braithwaite, A. C.; Wright, P. E.; Waters, T. N. *J. Inorg. Nucl. Chem.* **1975**, *37*, 1699−1674.
(41) Kurzak, K.; Kuzniarska-Biernacka, I.; Kurzak, B.; Jezierska, J. *J. Solution Chem.* **2001**, *30*, 709−731.

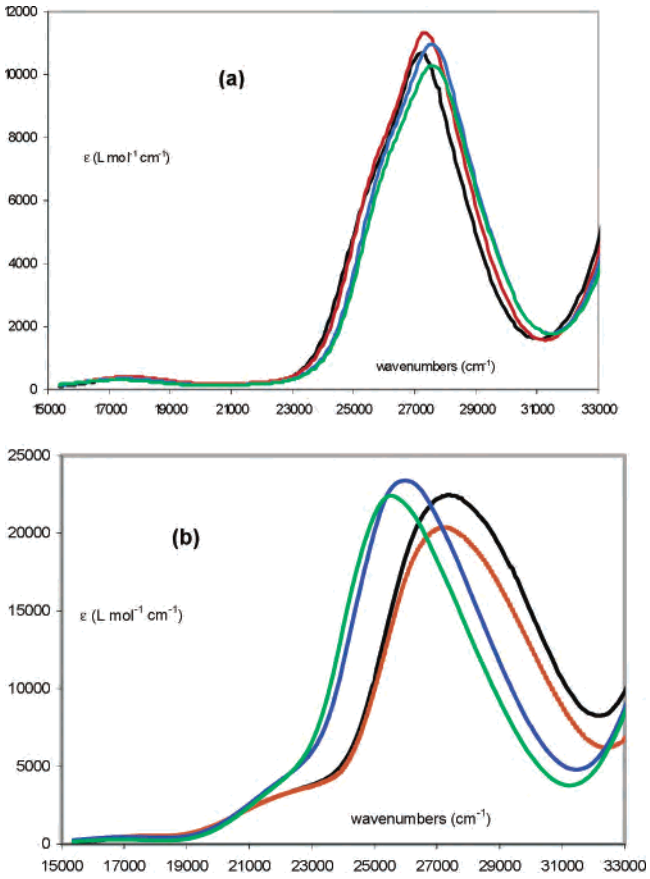

Figure 7. Electronic spectra of compounds **1a** (a) and **1h** (b) in different solvents: black, $CHCl_3$; red, CH_2Cl_2; blue, *N*,*N*-dimethylformamide (DMF); green, DMSO.

Table 5. Deconvolutions of First Near-UV Band of the Spectra in $CHCl_3$ Solutions[a]

compd	LMCT/cm^{-1} (ϵ/L mol^{-1} cm^{-1})	$\pi-\pi^*$/cm^{-1} (ϵ/L mol^{-1} cm^{-1})	$\pi-\pi^*$/cm^{-1} (ϵ/L mol^{-1} cm^{-1})
1a	25 262 (1550)	27 201 (8000)	27 228 (2700)
1b	24 780 (800)	26 725 (8400)	26 845 (1900)
1c	23 096 (2000)	26 373 (8600)	26 288 (2290)
1d	22 304 (2440)	26 924 (4450)	25 722 (2720)
1e	25 476 (4960)	27 314 (16 990)	29 275 (11 340)
1f	no	no	no
1g	23 149 (2310)	26 486 (8770)	28 214 (19 470)
1h	22 446 (3130)	26 238 (8320)	28 369 (19 750)
1i	no	26 795 (10 360)	no
1j	no	26 402 (9800)	no
1k	23 150 (2540)	26 544 (6950)	no
1l	22 096 (3090)	26 200 (8110)	no
1m	no	25 997 (8530)	27 824 (20 780)
1n	no	25 928 (7780)	27 973 (20 290)
1o	23 440 (2890)	25 955 (7970)	28 015 (19 430)
1p	22 643 (4040)	25 890 (7850)	27 816 (17 860)

[a] no = not observed.

Simulation of the Electronic Absorption Spectra of Complexes 1a, 1c, 1e, 1h, and 1i. To confirm the assignments of the bands, we performed theoretical calculations on the low-lying excitations of selected compounds, i.e., [Cu(salen)] (**1a**), its derivatives with OMe (**1c**), with NO_2 (**1e**), with both NO_2 and NMe_2 groups (**1h**), and the unsubstituted complex with the tn bridge (**1i**). The observed underestimations (2000−5000 cm^{-1}) of the computed excitation energies with respect to the experimental values are in the range expected for TDDFT calculations on UV−visible transitions

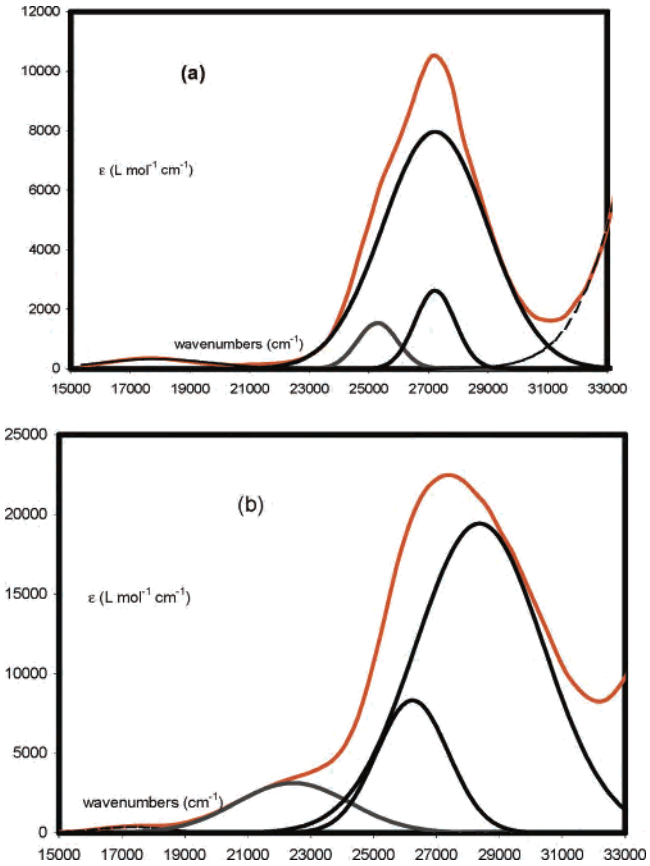

Figure 8. Deconvolutions of the near-UV band of the chloroform solution spectra of **1a** (a) and **1h** (b). The red lines are the experimental spectra.

of metal-containing systems.[42,43] Details of the calculated lower energy transition of the five complexes in $CHCl_3$ are reported in Table 6.

In all cases, the most significant (i.e., with the associated oscillator strength >0.02) transition at lower energy was unambiguously imputable to the excitation of one electron from a singularly occupied molecular orbital, describing the σ system of the ligand, to the lowest unoccupied molecular orbital (LUMO), principally localized on the metal, i.e., a LMCT transition. The nature of this transition was confirmed by all of the computational approaches used (type of exchange-correlation functional, inclusion, or not of the solvent).

The subsequent transitions, unlike the low-energy one, depend not only on the complex under examination but also on the chosen computational approach. They are roughly grouped in two different regions of the spectrum and involve essentially different portions of the molecular π system ($\pi \rightarrow \pi^*$ transitions). In all cases, the major contributions to these transitions derive from excitations from both the aromatic moieties of the complexes toward the NO_2 group, when present, and/or the C═N groups.

The introduction of one OMe group in [Cu(salen)] keeps essentially unvaried the position of the LMCT band (compare **1c** with **1a**), while the presence of one NO_2 group determines a shift to higher energies of about 800 cm^{-1} (compare **1e** with **1a**). A similar shift was obtained also in the computed spectrum of **1h**. While the shift due to the presence of NO_2 reproduces that observed experimentally (see Table 5), the donor groups OMe and NMe_2 do not show any influence on the position of the LMCT transition, which, instead, are red-shifted in the experimental spectra. This lack of influence was confirmed also by repeating spectra calculations on **1h** with both a much larger basis set, i.e., the ADF "ET-pVQZ" basis set, and a different exchange-correlation functional, such as the LB94 functional.[44] So, the reason for the scarce influence of the donor groups on the position of the computed LMCT transition still remains unclear.

From Table 6, a significant increase of the LMCT transition oscillator strengths f is observed on going from the unsubstituted [Cu(salen)] to the OMe-substituted complex **1c** and even more to the nitro derivatives **1e** and **1h**. This is in agreement with the results of solvatochromism studies (see below), and it is a consequence of increasing transition dipole moments, μ_{eg}, that is, of the degree of CT associated with the transition.

Table 6 reports also an analysis of the principal MO → MO contributions to the LMCT transition. In complexes **1a**, **1c**, **1e**, and **1h**, the orbitals involved in the major contribution are essentially localized on the metal and the donor O atoms, while lower significant contributions involve π orbitals delocalized in different ways on the molecule. Note the asymmetric distribution of the MOs of the major contribution in complexes **1c**, **1e**, and **1h**, which reflects the different polarizations of the molecules.

This analysis indicates that CT occurs along two possible directions, that is, the y axis (from donor O to metal atoms) and the x axis (from donor to acceptor moieties). Moreover, the direction of CT along y is the same as μ_y, while that along x is opposite to μ_x, implying a reduction along y and an enhancement along the x axis of the molecular polarization. As a result, for complexes **1a**, where CT along x is absent, and **1c**, where it is negligible, we expect that the LMCT transition is associated with a decrease of the molecular dipole moment ($\Delta\mu_{eg} < 0$). On the other hand, the presence of NO_2 in **1e** and **1h** is expected to render the CT along x the predominant contribution, with a concomitant increase in polarization ($\Delta\mu_{eg} > 0$) associated with this transition.

The LMCT transition of tn complex **1i**, which in the experimental spectrum is too weak to be properly deconvoluted, is found at an energy similar to that of **1a**, but it is characterized by a slightly larger transition dipole moment. Moreover, a different localization scheme of the orbitals involved in the transition is observed, owing to the large deviation from planarity. In this compound, the occupied orbital involved in the major contribution to the LMCT transition is delocalized on the whole molecule (with exclusion of the tn bridge), while the orbital localized on the metal and the donor O atoms is involved only in the

(42) Ciofini, I.; Lainé, P. P.; Bedioui, F.; Adamo, C. *J. Am. Chem. Soc.* **2004**, *126*, 10763−10777.
(43) Petit, L.; Adamo, C.; Russo, N. *J. Phys. Chem. B* **2005**, *109*, 12214−12221.
(44) In this case, the transitions were all translated toward lower energies.

Table 6. Computed Data for the LMCT Transition of Complexes **1a**, **1c**, **1e**, **1h**, and **1i** in $CHCl_3$: Energies (E), Oscillator Strengths (f), Transition Dipole Moments (μ_{eg}), and Analysis of the More Important Contributions to the Transition

				major contribution			secondary contribution	
compd	E (cm^{-1})	f	μ_{eg} (D)	weight	occupied orbital population[a]	virtual orbital (LUMO) population[a]	weight	involved orbitals
1a [en, H, H]	19 729	0.026	1.68	0.71	24.3% p_y O 24.3% p_y O 19.6% $d_{x^2-y^2}$	47.3% d_{xy} 7.1% p_y O 7.1% p_y O	0.27[b]	$\pi_{ar} \rightarrow \pi^*_{C=N}$
1c [en, H, OMe]	19 770	0.034	1.92	0.52	24.4% p_y O(OMe) 23.9% p_y O(H) 19.3% $d_{x^2-y^2}$	46.4% d_{xy} 7.4% p_y O(H) 6.8% p_y O(OMe)	0.29[b]	$\pi_{ar-OMe} \rightarrow \pi^*_{C=N(H)}$[c,d]
1e [en, NO_2, H]	20 557	0.113	3.41	0.56	26.6% p_y O(H) 20.9% p_y O(NO_2) 19.4% $d_{x^2-y^2}$	47.0% d_{xy} 8.2% p_y O(H) 5.9% p_y O(NO_2)	0.29[b]	$\pi_{ar(H)} \rightarrow \pi^*_{C=N(NO2)}$[e]
1h [en, NO_2, NMe_2]	20 536	0.124	3.59	0.78	26.1% p_y O(NMe_2) 20.6% p_y O(NO_2) 19.1% $d_{x^2-y^2}$	47.1% d_{xy} 8.2% p_y O(NMe_2) 5.9% p_y O(NO_2)	0.05	$\pi_{ar(NMe2)} \rightarrow$ LUMO[f]
1i [tn, H, H]	20 034	0.035	1.93	0.73	highly delocalized	22.5% d_{z^2} 8.9% d_{xy} 8.8% d_{xz}	0.13	$\sigma_{Cu-O} \rightarrow$ LUMO[g]

[a] Singularly occupied molecular orbitals. [b] Contribution from both α and β electrons. [c] $\pi^*_{C=N(H)}$, $\pi_{ar(NMe2)}$, etc., are the molecular orbitals of π symmetry principally localized, respectively, on the C═N bond on the side of the unsubstituted sal moiety, on the aromatic system on the side of the NMe_2 group, etc. [d] The following contribution (weight 0.12) corresponds to excitation $\pi_{ar(H)} \rightarrow \pi^*_{C=N(OMe)}$. [e] The following contribution (weight 0.08) corresponds to excitation $\pi_{ar(H)} \rightarrow \pi^*_{C=N(H)}$. [f] The following contribution (weight 0.10) corresponds to excitation $\pi_{ar-NMe2} \rightarrow \pi^*_{ar(NO2)}$. [g] Excitation from a singularly occupied molecular orbital (15% $d_{x^2-y^2}$, 14% p_z O, 11% p_y O) to the same virtual orbital (LUMO) of the principal contribution.

Table 7. Position of the LMCT Bands (cm^{-1}) in the Various Solvents and NLO Parameters

solvent, $E_T(30)$[a]	**1a**	**1c**	**1h**	**1k**	**1l**	**1o**	**1p**
ethyl acetate, 38.1	25 327	23 205	22 538	23 165	22 126	23 577	22 811
$CHCl_3$, 39.1	25 262	23 096	22 446	23 150	22 096	23 440	22 643
CH_2Cl_2, 40.7	25 476	23 330	22 296	23 322	22 163	23 374	22 642
dichloroethane, 41.3	25 527	23 347	22 283	23 330	22 220	23 229	22 601
DMF, 43.8	25 770	23 592	22 148	23 576	22 354	22 764	22 535
DMSO, 45.1	25 930	23 640	22 026	23 663	22 382	22 700	22 500
CH_3CN, 45.6	25 660	23 575	22 464	23 508	22 330	23 509	22 699
μ_{eg} (D)	1.48	1.94	2.66	2.14	3.10	2.62	4.15
$\Delta\mu_{eg}$ (D)	−2.84	−5.56	1.1	−2.1	−2.7	2.4	1.4
dispersion factor, $F(\omega)$	1.26	1.33	1.35	1.33	1.37	1.32	1.35
$\beta_{0,static}$ (10^{-30} cm^5 esu^{-1})	−0.4	−1.5	0.8	−1.6	−2.0	1.8	1.0
β_{CT} (10^{-30} cm^5 esu^{-1})	−0.5	−2.0	1.1	−2.1	−2.7	2.4	1.4

[a] $E_T(30)$ (kcal mol^{-1}) is the Reichardt polarity parameter.[46]

secondary contribution. In both contributions, the virtual orbital is the LUMO, which is principally localized on the metal atom.

NLO Properties. Although the NLO responses of our compounds (see below) are in the range reported for other Schiff base complexes,[5−7] we have studied in some detail the effects of the modulation of the charge asymmetry on various NLO parameters, in view of future applications.

NLO Parameters from Solvatochromic Experiments. The positions of the LMCT bands in various solvents of the compounds, for which reliable deconvolutions of the near-UV absorption could be made, are reported in Table 7, together with the NLO parameters obtained by the solvatochromism experiments. There are some anomalies in the trend of the absorption maxima with solvent polarity (CH_3CN and ethyl acetate), but a general trend is easily observed.[45]

The hyperpolarizability values were evaluated according to the "two-state" model,[19] using the same LASER frequency of the EFISH experiments (1.907 μm, 5244 cm^{-1}) and utilizing the equations found in the literature.[21−23] With this model, it is possible to calculate β_{CT}, i.e., the value of β along the direction of the CT transition (see the Experimental Section).

The hypsochromic shift of the LMCT transition of the compounds void of the nitro group with increasing solvent polarity is associated with a decrease of the dipole moment on passing from the ground to excited state (i.e., a negative $\Delta\mu_{eg}$), which corresponds to a negative value of β_{CT}. The opposite effect is observed for the compounds with the NO_2 group, which causes a change of the sign of β_{CT}. The absolute values of β_{CT} are not high because these bands correspond to transitions that, according to the above-described spectral simulations, involve orbitals in close proximity to each other, being localized on Cu and donor O atoms.

(45) Anomalies of the plot of absorption maxima versus polarity parameters have been observed in other instances.[4e] See also: (a) Alain, V.; Redoglia, S.; Blanchard-Desce, M.; Lebus, S.; Lukaszuk, K.; Wortmann, R.; Gubler, U.; Bosshard, C.; Guenter, P. *Chem. Phys.* **1999**, *245*, 51−57. (b) Averseng, F.; Lacroix, P. G.; Malfant, I.; Dahan, F.; Nakatani, K. *J. Mater. Chem.* **2000**, *10*, 1013−1018. We believe this behavior depends on the polarity scale used and/or on solvation effects.

(46) (a) Dimroth, K.; Reichardt, C.; Siepman, T.; Bohlman, F. *Liebigs Ann. Chem.* **1963**, *661*, 1−37. (b) Abboud, J.-L. M.; Notario, R. *Pure Appl. Chem.* **1999**, *71* (4), 645−718.

Table 8. EFISH and Static Computed NLO Parameters[a]

	experimental (EFISH)		computed values						
compd	$\mu_g\beta_{vec}$	β_{vec}	β_x	β_y	β_z	β_{tot}	β_{vec}	$\mu_g\beta_{vec}$	θ (deg)
1a (H, H, en)	108	18	0.0	−11.8	0.0	11.8	−11.8	−72.2	180.0
1b (H, Me, en)	268	45	2.4	−12.4	0.0	12.6	−12.2	−73.0	169.8
1c (H, OMe, en)	205	42	7.6	−11.6	0.0	13.8	−11.1	−54.3	147.2
1d (H, NMe_2, en)			8.4	−15.7	4.0	18.3	−14.4	−88.8	149.1
1e (NO_2, H, en)	540	55	26.2	−12.7	−0.3	29.1	12.8	125.1	115.9
1f (NO_2, Me, en)			31.7	−12.8	−0.5	34.2	17.9	181.1	112.0
1g (NO_2, OMe, en)	493	51	40.0	−11.8	−0.2	41.7	27.3	262.1	106.4
1h (NO_2, NMe_2, en)	672	62	46.4	−16.5	3.8	49.4	28.6	310.9	109.5
1i (H, H, tn)	310	53	−1.7	−12.1	−0.2	12.3	−12.1	−71.3	170.0
1k (H, OMe, tn)	479	104							
1l (H, NMe_2, tn)	598	106							
1m (NO_2, H, tn)	540	58	21.2	−10.9	3.4	24.1	10.1	104.2	116.9
1p (NO_2, NMe_2, tn)	560	50							

[a] EFISH data obtained with laser irradiation at $\lambda = 1.907$ μm. β values in 10^{-30} cm^5 esu^{-1} and $\mu_g\beta_{vec}$ in 10^{-30} D cm^5 esu^{-1}. 10% errors. θ is the angle between β_{tot} and the y axis; see text and Figure 6.

EFISH Measurements. Table 8 reports the NLO properties of selected compounds, obtained by the EFISH technique, with β_{vec} evaluated using the computed μ_g values. These data refer to 5×10^{-4} mol L^{-1} $CHCl_3$ solutions, i.e., in a range where the spectra follow the Lambert−Beer law. The lower responses obtained at higher concentrations are likely to be due to the presence of intermolecular associations because the head-to-tail nature of these associations, evidenced by the X-ray structures, gives rise to partial cancellation of the charge asymmetry.

The absolute $\mu_g\beta_{vec}$ and β_{vec} values are in the (100−700) $\times$ 10^{-30} D cm^5 esu^{-1} and (18−115) $\times$ 10^{-30} cm^5 esu^{-1} ranges, respectively, similar to those found for other Schiff base complexes.[5−7] The highest figures of $\mu_g\beta_{vec}$ are displayed by the NO_2−NMe_2 derivatives (**1h** and **1p**); however, their β_{vec} values are not the highest because this kind of substitution gives rise also to a large μ_g.

Computed Hyperpolarizabilities. The EFISH experiment samples the second-order NLO response along the direction of the dipole moment, β_{vec}.[47] However, application of an electric field may induce intramolecular CT also in other directions, as happens in many organometallic architectures.[48] We have therefore computed the full β_{tot} vector to gain more complete information on the second-order response of the molecules. The magnitude of this vector reduces to β_{vec} when the CT is unidirectional and oriented along the dipole moment.

In the framework of the DFT approach, several methods have been implemented in computer programs for obtaining both the static and dynamic nonlinear coefficients β_{ijk}, but, as a rule, they are currently restricted to closed-shell systems. For open-shell systems, such as the copper(II) complexes, the finite-field method represents one of the few theoretical approaches for ab initio calculation of the static components of β.

In Table 8, the β_i, β_{tot}, and β_{vec} quantities, derived from the computed static tensor β, are reported. These figures are interesting because they provide information on the potential modulation of the relative magnitude of the β components in our compounds and, accordingly, the modulus and direction of β_{tot}. In the case of the parent [Cu(salen)], β_{tot} is obviously parallel to the y axis, as is μ_g, but the two vectors point toward opposite directions, in agreement with the simulated spectrum, giving rise to a negative β_{vec} projection. The unsymmetrical introduction of D and/or A groups on the two sides of the molecules generates a positive x component of both vectors, tilting their direction with respect to the y axis (in the following, the angle between y and β_{tot} will be described as θ; see Figure 6). The presence of only a D group (compounds **1a**−**1d**) generates relatively small x components, maintaining the angle between β_{tot} and μ_g (i.e., $\theta-\phi$) larger than 90° and β_{vec} negative. The larger variations are, once more, observed with NO_2, which produces very large and positive β_x components, while keeping the β_y's almost unvaried. As a result, larger magnitudes of β_{tot} are obtained, with a significant increase along the series **1e**−**1h**. In the same time, the concomitant increase of β_x and μ_x components renders $\theta-\phi$ smaller than 90°, giving rise to positive β_{vec} projections.

The increase of the computed absolute values of the $\mu_g\beta_{vec}$ products reproduces acceptably the experimental trend, in particular for what concerns the effect of the NO_2 group. The calculated $|\beta_{vec}|$ values are clearly smaller than the experimental values because the former have been obtained with a static electric field. However, there is a disagreement of the sign of β_{vec}, with the EFISH measurements in the series **1a**−**1d**.[49] We recall that the sign of computed β_{vec} values is determined by the relative predominant direction (i.e., x or y) of the CT. In compounds **1e**−**1h**, there is a sharp prevalence of the x component over the y component of β_{tot}, while for **1a**−**1d**, the two components are similar, and the prevalence of one over the other is sensitive to the chosen

(47) $\beta_{vec} = \sum_i(\mu_i\beta_i)/\mu_g$, where $\beta_i = \beta_{iii} + (1/3)\sum_{j\neq i}(\beta_{ijj} + \beta_{jij} + \beta_{jji})$ are the components of the total intrinsic quadratic hyperpolarizability, β_{tot}.[1g]

(48) Kanis, D. R.; Ratner, M. A.; Marks, T. J. *J. Am. Chem. Soc.* **1992**, *114*, 10338−10357.

(49) This result has been confirmed also by analytical coupled perturbed Hartree−Fock CPHF/6-31++G** calculations[24] on **1f** as a test. Discrepancies of the sign between calculated and experimental β_{vec} values have been reported in other instances. For instance, see: (a) Shelton, P. D.; Rice, J. E. *Chem. Rev.* **1994**, *94*, 3−29. (b) Bruschi, M.; Fantucci, P.; Pizzotti, M. *J. Phys. Chem. A* **2005**, *109*, 9637−9645.

theoretical approach, including, in particular, treatment of solvent effects. Further work in this direction is in progress.

On the other hand, the signs of the computed β_{vec}'s agree with those of the β_{CT}'s as obtained from solvatochromic experiments (see Table 7). In fact, both approaches predict that, for compounds void of the nitro group, the CT direction is opposite to that of the dipole moment, while in the presence of this group, it occurs in the same direction. The solvatochromism experiments appear, however, to largely underestimate the order of magnitude of the β_{CT}'s, probably because of (i) the simplicity of the "two-state" model, (ii) the fact that we have considered only the lowest energy transition, and (iii) the intrinsic uncertainties of the deconvolution procedure.

Conclusions

In this paper, we have described an approach to the modulation of the electronic and NLO properties of [Cu(salen)] analogues, with a push−pull structure along the *x* axis. Combined experimental and DFT theoretical studies have shown that the most relevant effects on the properties of the complexes are determined by the introduction of the NO_2 group in one sal moiety. Such unsymmetrical substitution increases significantly the magnitudes of μ_g and β_{tot}. On the other hand, the donor groups investigated here (Me, OMe, and NMe_2) are less effective in modulating μ_g but are able to enhance β_{tot}.

To understand the different effects of the unsymmetrical substitutions on the NLO properties of these complexes, we have performed a careful analysis, including deconvolution procedures, of their electronic spectra, which allowed the identification of a LMCT absorption band controlling the NLO response. The nature of such a transition has been fully confirmed by TDDFT calculations, which, in particular, have evidenced the presence and relative importance of two competitive directions of CT within the complexes: one from donor O to Cu atoms and the other from donor to acceptor groups. The predominance of one contribution over the other accounts for the sign of β_{CT} (negative in the absence of NO_2 and positive otherwise), as obtained by solvatochromism studies. It is to be remarked that, to the best of our knowledge, the theoretical investigation of the present study represents one of the first computational analyses of the second-order NLO response of open-shell transition-metal complexes.

Although the β values of compounds **1** are in the range reported for similar compounds, the charge asymmetry originated by the unsymmetrical substitution described here allows a great freedom in the design of metal complexes with tunable properties: a proper choice of the substituents can give rise to a great possibility of modulating parameters such as μ_g and β. Moreover, although here we have used only en and tn, our approach is independent of the structure of the diamine, further increasing the possibility of modulations.

As to the influence on coordination bond lengths of the unsymmetrical substitutions, both crystal structures and DFT geometry optimizations have shown that only NO_2 has a relevant effect, and mainly on the Cu−O bonds. This may be originated by the fact that we have examined 5-substituted salicyilaldehydes (i.e., para to the phenolato O atom), a position chosen to produce a component of the charge asymmetry along the *x* direction. However, it has previously been shown that it is this substitution (rather than substitution in position 4) that has some influence on other properties of [Cu(salen)] analogues, such as their oxidation potential.[50]

Finally, metal complexes of unsymmetrically substituted salen analogues may be of interest also in other fields, such as catalysis and models of bioinorganic systems,[51] because the charge asymmetry and the possible fine-tuning of the electronic properties, originating from the different substitutions, can create active sites with potential regioselective molecular recognition, as suggested by the head-to-tail arrangements of the molecules found in the crystal structures.

Acknowledgment. We thank S. Di Bella, University of Catania, for helpful discussion and R. Ugo and M. Pizzotti, University of Milan, for encouragement. This work has been supported by the FIRB 2003 project "molecular compounds and hybrid nanostructured materials with resonant and non resonant optical properties for photonic devices".

Supporting Information Available: Structural data for compounds **1g**, **1n**, **1o**, and **1p** (CIF format). This material is available free of charge via the Internet at http://pubs.acs.org.

IC0613513

(50) Pasini, A.; Bernini, E.; Scaglia, M. *Polyhedron* **1996**, *24*, 4461−4467.
(51) For instance, see: (a) Huber, A.; Mueller, L.; Elias, H.; Klement, R.; Valko, M. *Eur. J. Inorg. Chem.* **2005**, 1459−1467. (b) Kleij, A. W.; Tooke, D. M.; Spek, A. L.; Reek, J. N. H. *Eur. J. Inorg. Chem.* **2005**, 4622−4633. (c) Zhu, B.; Ruang, W.; Zhu, Z. *Acta Crystallogr., Sect. E* **2004**, *E60*, m634−m636. (d) Tao, R.-J.; Mei, C.-Z.; Zang, S.-Q.; Wang, Q.-L.; Niu, J.-Y.; Liao, D.-Z. *Inorg. Chim. Acta* **2004**, *357*, 1985−1990. (e) Boghaei, D. N.; Mohebi, S. *Tetrahedron* **2002**, *58*, 5357−5366.